

Molecular Quantum Dynamics: A Quantum Computing Perspective

Published as part of the Accounts of Chemical Research special issue “*Direct Dynamics of Chemical Processes and Pathways*”.

Pauline J. Ollitrault,[†] Alexander Miessen,[†] and Ivano Tavernelli*



Cite This: *Acc. Chem. Res.* 2021, 54, 4229–4238



Read Online

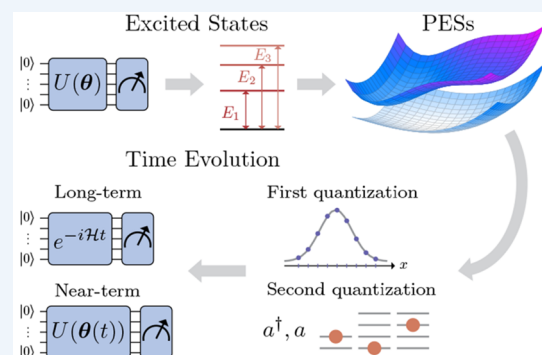
ACCESS |

Metrics & More

Article Recommendations

CONSPECTUS: Simulating molecular dynamics (MD) within a comprehensive quantum framework has been a long-standing challenge in computational chemistry. An exponential scaling of computational cost renders solving the time dependent Schrödinger equation (TDSE) of a molecular Hamiltonian, including both electronic and nuclear degrees of freedom (DOFs), as well as their couplings, infeasible for more than a few DOFs. In the Born–Oppenheimer (BO), or adiabatic, picture, electronic and nuclear parts of the wave function are decoupled and treated separately. Within this framework, the nuclear wave function evolves along potential energy surfaces (PESs) computed as solutions to the electronic Schrödinger equation parametrized in the nuclear DOFs. This approximation, together with increasingly elaborate numerical approaches to solve the nuclear time dependent Schrödinger equation (TDSE), enabled the treatment of up to a few dozens of degrees of freedom (DOFs). However, for particular applications, such as photochemistry, the BO approximation breaks down. In this regime of non-adiabatic dynamics, solving the full molecular problem including electron–nuclear couplings becomes essential, further increasing the complexity of the numerical solution. Although valuable methods such as multiconfigurational time-dependent Hartree (MCTDH) have been proposed for the solution of the coupled electron–nuclear dynamics, they remain hampered by an exponential scaling in the number of nuclear DOFs and by the difficulty of finding universal variational forms.

In this Account, we present a perspective on novel quantum computational algorithms, aiming to alleviate the exponential scaling inherent to the simulation of many-body quantum dynamics. In particular, we focus on the derivation and application of quantum algorithms for adiabatic and non-adiabatic quantum dynamics, which include efficient approaches for the calculation of the BO potential energy surfaces (PESs). Thereafter, we study the time-evolution of a model system consisting of two coupled PESs in first and second quantization. In a first application, we discuss a recently introduced quantum algorithm for the evolution of a wavepacket in first quantization and exploit the potential quantum advantage of mapping its spatial grid representation to logarithmically many qubits. For the second demonstration, we move to the second quantization framework and review the scaling properties of two alternative time-evolution algorithms, namely, a variational quantum algorithm (VQA) (based on the McLachlan variational principle) and conventional Trotter-type evolution (based on a Lie–Trotter–Suzuki formula). Both methods clearly demonstrate the potential of quantum algorithms and their favorable scaling compared to the available classical approaches. However, a clear demonstration of quantum advantage in the context of molecular quantum dynamics may require the implementation of these algorithms in fault-tolerant quantum computers, while their application in near-term, noisy quantum devices is still unclear and deserves further investigation.



KEY REFERENCES

- Ollitrault, P. J.; Kandala, A.; Chen, C.-F.; Barkoutsos, P. K.; Mezzacapo, A.; Pistoia, M.; Sheldon, S.; Woerner, S.; Gambetta, J. M.; Tavernelli, I. Quantum equation of motion for computing molecular excitation energies on a noisy quantum processor. *Phys. Rev. Res.* **2020**, 2, 043140.¹ This work describes a quantum algorithm to compute excited states of a molecular Hamiltonian

based on the evaluation of ground state expectation values.

Received: August 18, 2021

Published: November 17, 2021



- Ollitrault, P. J.; Mazzola, G.; Tavernelli, I. Nonadiabatic Molecular Quantum Dynamics with Quantum Computers. *Phys. Rev. Lett.* **2020**, *125*, 260511.² This work presents a novel quantum algorithm to simulate non-adiabatic quantum dynamics on a spatial grid with product formulas.
- Miessen, A.; Ollitrault, P. J.; Tavernelli, I. Quantum algorithms for quantum dynamics: a performance study on the spin-boson model, *arXiv preprint*, 2021, arXiv:2108.04258, <https://arxiv.org/abs/2108.04258>.³ This work reports on a scaling study comparing a time-dependent variational quantum algorithm and a Trotter-based evolution for different spin-boson models.

1. INTRODUCTION

Quantum dynamics is of particular relevance when studying nonequilibrium processes involving several potential energy surfaces (PESs) (e.g., after photoexcitation), where pure non-adiabatic quantum effects (such as internal conversion and intersystem crossing) become dominant. The quantum dynamics of molecular and solid-state systems deals with the solution of the combined electron and nuclear dynamics as described by the time dependent Schrödinger equation (TDSE). However, the exact solution of the corresponding “multicomponent” equations of motion (EOMs) for the total electron–nuclear, or simply molecular, wave function is a formidable task that can only be obtained for model systems with few electrons and nuclei in low dimensions.

The Born–Oppenheimer (BO) approximation provides a conceptual and operational strategy for solving this issue. In this case, the molecular wave function becomes a simple product of the nuclear and electronic wave functions with only the first one explicitly dependent on time. The Born–Huang (BH) expansion is widely used since it gives rise to the very intuitive picture of a nuclear wavepacket evolving along parametrized PESs corresponding to the electronic eigenenergies. The couplings between the different PESs are called non-adiabatic (or vibronic) couplings and mediate the transfer of amplitude among the states. Many numerical approaches for quantum dynamics in the extended BO picture^{4–6} have been developed and are, today, routinely employed in molecular simulations (in the adiabatic as well as non-adiabatic regimes using wavepackets or trajectory-based approaches). However, the accuracy is often sacrificed to lower the computational cost on traditional computers. Further insights into state-of-the-art quantum dynamics methods can be found in refs 7 and 8.

Alternatively, molecular quantum dynamics can also be expressed as a simple product of time-dependent electronic and nuclear wave functions. This formalism, first introduced by J. von Neumann and G. Hunter (see ref 9 and references therein), was recently further developed by Gross and co-workers⁹ and turned into a numerical algorithm for the simulation of non-adiabatic quantum processes.¹⁰ Interestingly, within this framework, a single, explicitly time-dependent PES describes the exact molecular quantum dynamics of the electron–nuclear wave function, where the two components are coupled through the action of a vector potential.⁹ Despite the clear conceptual advantage associated with this representation, the equations of motion (EOMs) are quite involved, hampering its deployment.

Today, quantum computing is emerging as a new computational paradigm for the simulation of quantum chemistry and

quantum physics with favorable scaling. A detailed introduction to quantum computing is given, for instance, in ref 11, as well as in refs 12 and 13 for more specific applications in quantum chemistry. In recent years, we have witnessed a fast growth of quantum algorithms for the solution of electronic structure problems for molecules^{13–15} and periodic¹⁶ or condensed phase systems,¹⁷ as well as for the calculation of time-dependent properties such as time correlation functions and molecular dynamics (MD).

Concerning combined electron–nuclear quantum dynamics, while formally possible and simple to formalize in second quantization, this approach remains beyond what can be currently achieved with state-of-the-art quantum computers. In fact, in order to keep the resources (number of qubits) within a reasonable boundary, current quantum algorithms are confined to the BO picture, adding non-adiabatic effects perturbatively (see section 4). For the same reasons, quantum algorithms for trajectory-based approaches are currently limited to the adiabatic case,¹⁸ although extensions to non-adiabatic situations are already within reach, especially after the development of algorithms for the calculation of excited states properties (see section 2.4). Due to these resource limitations, current quantum computing applications in chemistry focus mainly on simple molecules (with small basis sets) or simplified model systems. Although considerable improvements in quantum hardware are needed to go beyond the treatment of illustrative models, quantum algorithms already offer attractive scaling improvements.

Herein, we give our perspective on the design of algorithms to exploit the enormous potential of quantum computers and to solve efficiently, that is, with a polynomial scaling of the needed resources, the molecular TDSE. In particular, we present different visions for encoding the problem in quantum computers (first and second quantization formulations) as well as two approaches for the propagation of the nuclear wave function, one based on the McLachlan variational principle (MVP)¹⁹ and the other on the Trotter–Suzuki expansion of the unitary time-evolution operator.^{20,21} Finally, we compare them in several concrete applications and conclude on the potential of quantum advantage for quantum dynamics with near-term (noisy) and fault-tolerant (error corrected) quantum computers. This work is organized in the following way. First, we introduce quantum algorithms for the calculation of ground and excited PESs in section 2, which form the basis of adiabatic and non-adiabatic dynamics. In section 3, we then introduce a series of quantum algorithms for quantum dynamics. Finally, in sections 4 and 5, we present two applications, one on non-adiabatic dynamics formulated in first quantization and the other on a spin-boson system in second quantization. Section 6 concludes with discussing the potential of quantum algorithms and their future role in molecular quantum dynamics.

2. CALCULATION OF THE POTENTIAL ENERGY SURFACES

Within the BO picture, the first step toward simulating MD resides in calculating the PESs, that is, finding the eigenstates of the electronic Hamiltonian. While this task remains challenging with traditional approaches, quantum computing methods present themselves as possibly efficient alternatives. In this section, we give a short summary of the main quantum algorithms for electronic structure calculations in first and second quantization.

2.1. Mapping of a Many-Electron System to a Workable Qubit Representation

Problems in first quantization naturally discretize space on a grid, and the grid points are encoded in the basis states of qubits. For instance, for an N -electron system, discretizing each of the three spatial dimensions into P points requires storing $P^{3N} \times 2^N$ complex amplitudes. This makes the classical simulation intractable for systems with more than a few particles. However, by encoding the points in the binary representation of the qubit basis, only $(3 \log_2(P) + 1)N$ qubits are needed to store the same information. A drawback of this approach is that it suffers from a large qubit number overhead²² compared to the basis-set approach outlined in the next paragraph. As a result, grid-based approaches are largely under-studied compared to algorithms employing basis-sets. Nonetheless, they enjoy interesting features such as a better scaling in the number of qubits, the lack of classical preprocessing, and a reduced number of measuring bases. Therefore, in section 4, we use them to simulate non-adiabatic quantum dynamics.

Alternative to a grid representation, the problem may be encoded using basis functions (orbitals), where their occupations are mapped to qubit states and the Hamiltonian is rewritten in second quantization. In practice, qubit states then represent sets of orbitals. Equivalently, creation and annihilation operators, a_i^\dagger and a_i , must be mapped to spin (Pauli) operators, $\sigma_i^\pm = (\sigma_i^x \pm i\sigma_i^y)/2$, obeying the correct spin-statistics.

2.2. Quantum Algorithms for Ground State Calculations

A promising class of algorithms for near-term quantum computing are variational quantum algorithms (VQAs). They introduce an iteration loop between a quantum and a classical processor, drastically reducing the quantum gate cost. The quantum processor prepares a variational trial state $|\psi(\theta)\rangle$, where θ is a vector of variational parameters encoded in the quantum circuit as single-qubit rotation angles, $R_\mu(\theta) = \exp(-i\theta\sigma^\mu/2)$, with σ^μ ($\mu = x, y, z$) being a Pauli matrix. An observable is then measured on the quantum state, and the result is passed to the classical computer, where new parameters are computed by evaluating a problem-specific cost function. The new parameters are fed back to the quantum processor for the next iteration, and the procedure is repeated until reaching convergence.

The most popular VQA, which is particularly relevant here, is the variational quantum eigensolver (VQE).^{23,24} Relying on the Rayleigh–Ritz variational principle, VQE approximates, for example, the ground state of a Hamiltonian,

$$\langle\psi(\theta)|\mathcal{H}|\psi(\theta)\rangle \geq E_0 \quad (1)$$

where E_0 is the ground state energy of the Hamiltonian \mathcal{H} . In the general VQA framework presented above, the cost function simply becomes the energy expectation value of the trial state, and the parameters are classically optimized to minimize the energy. Note that the energy gradient can also be measured on the trial state,^{18,25,26} which some optimizers require as input.

2.3. Ansätze for the Variational Preparation of a Many-Body Wave Function

A crucial aspect of VQAs is the choice of the wave function ansatz. For the algorithm to be efficient and yield accurate results, the variational form has to be flexible enough to reproduce the correct state while maintaining low numbers of parameters and quantum gates. Ideally, the parameter space

should scale polynomially with the system size and lead to a well-behaved classical optimization. Satisfying these constraints is a nontrivial task and, hence, finding variational forms for approximating electronic ground states with VQE is an active field of research.

The unitary coupled cluster (UCC) ansatz,^{23,27–29} inspired from the standard coupled cluster (CC) method,³⁰ is certainly the most popular ansatz for electronic structure calculations. In ref 31, we showed that the variational nature of the quantum implementation can cure some of the issues associated with the classical, canonical, projective implementation of CC. However, despite its theoretical success, concrete applications of unitary coupled cluster (UCC) remain difficult as it comprises multiple expensive nonlocal operations, even though several approximations have been proposed to reduce its initial gate complexity, $O(N_{\text{orbitals}}^3 N_{\text{electrons}}^2)$ ^{31–33}

An alternative approach for designing wave function ansätze suited to near-term quantum computing is heuristic and tailored to the hardware. These *hardware efficient* ansätze^{13,15,34} comprise alternating layers of single-qubit rotations and entangling blocks adjusted to the hardware connectivity. However, there is no guarantee that such variational forms can reproduce the desired state with arbitrary accuracy.

In ref 35, we showed how to improve variational wave functions through nonunitary operations without increasing the circuit depth.

2.4. Quantum Algorithms for Excited State Calculations

The calculation of molecular excited state properties constitutes an additional challenge for both classical and quantum electronic structure algorithms.

In ref 1, we proposed a quantum algorithm for the calculation of the molecular excited states, which relies solely on the optimization of the ground state wave function, followed by the measurement of “excited” matrix elements. Alternative algorithms are reported in the literature, see, for instance, refs 36–40. Within this approach, excited states $|n\rangle$ are generated by applying an excitation operator of the general form $O_n^\dagger = |n\rangle\langle 0|$ to the ground state $|0\rangle$ of the system, where $|n\rangle$ is the shorthand notation for the n^{th} excited state of the electronic structure Hamiltonian. The excitation energies $E_{0n} = E_n - E_0$ can then be expressed as

$$E_{0n} = \frac{\langle 0|[O_n, \mathcal{H}, O_n^\dagger]|0\rangle}{\langle 0|[O_n, O_n^\dagger]|0\rangle} \quad (2)$$

where $[A, B] = AB - BA$ and $[A, B, C] = \frac{1}{2}\{[[A, B], C] + [A, [B, C]]\}$ are the commutator and double commutator, respectively. The EOM approach aims to find approximate solutions to eq 2 by expressing O_n^\dagger as a linear combination of basis excitation operators with variable expansion coefficients. The excitation energies are then obtained through the minimization of eq 2 in the coefficient space, leading to the following pseudoeigenvalue problem,

$$\begin{pmatrix} \mathbf{M} & \mathbf{Q} \\ \mathbf{Q}^* & \mathbf{M}^* \end{pmatrix} \begin{pmatrix} \mathbf{X}_n \\ \mathbf{Y}_n \end{pmatrix} = E_{0n} \begin{pmatrix} \mathbf{V} & \mathbf{W} \\ -\mathbf{W}^* & -\mathbf{V}^* \end{pmatrix} \begin{pmatrix} \mathbf{X}_n \\ \mathbf{Y}_n \end{pmatrix} \quad (3)$$

where

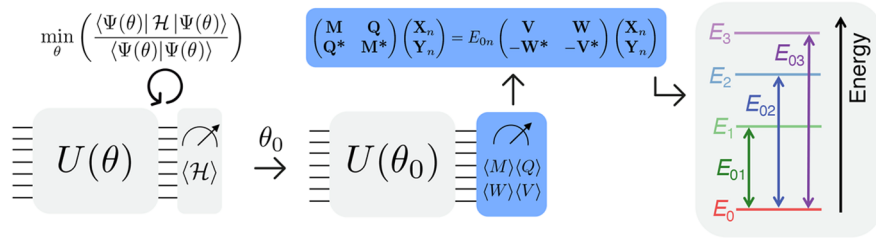


Figure 1. Graphical representation of the qEOM algorithm. Reproduced with permission from ref 1. Copyright 2020 American Physical Society.

$$M_{\mu_a \nu_\beta} = \langle 0 | [(\mathbf{E}_{\mu_a}^{(\alpha)})^\dagger, \mathcal{H}, \mathbf{E}_{\nu_\beta}^{(\beta)}] | 0 \rangle$$

$$Q_{\mu_a \nu_\beta} = -\langle 0 | [(\mathbf{E}_{\mu_a}^{(\alpha)})^\dagger, \mathcal{H}, (\mathbf{E}_{\nu_\beta}^{(\beta)})^\dagger] | 0 \rangle$$

$$V_{\mu_a \nu_\beta} = \langle 0 | [(\mathbf{E}_{\mu_a}^{(\alpha)})^\dagger, \mathbf{E}_{\nu_\beta}^{(\beta)}] | 0 \rangle$$

$$W_{\mu_a \nu_\beta} = -\langle 0 | [(\mathbf{E}_{\mu_a}^{(\alpha)})^\dagger, (\mathbf{E}_{\nu_\beta}^{(\beta)})^\dagger] | 0 \rangle$$

Here, $\mathbf{E}_{\mu_a}^{(\alpha)}$ are the basis excitation operators expressed as simple products of raising and lowering operators, a^\dagger and a , of order α and with μ_α a collective index for all one-electron orbitals involved in the excitation. Furthermore, the vectors \mathbf{X}_n , \mathbf{Y}_n comprise all variational expansion coefficients of O_n^\dagger . The rank of the matrices equals the number of excitations included in the expression of the operator O_n^\dagger (which can be truncated to keep the scaling polynomial with the system size).¹ The eigenvalues of eq 3 can therefore be evaluated classically. In particular, quantum advantage could be achieved through the efficient measurement of each matrix element in the EOM generalized eigenvalue problem. A graphical representation of this procedure published under the name of quantum-EOM (qEOM), is given in Figure 1.

We applied the method to the calculation of the excited states of several small molecules, yielding (simulated) excitation energies within chemical accuracy (≤ 1.5 mhartree). Moreover, we also applied the algorithm on a quantum computer⁴¹ to calculate the excitation energies of lithium hydride in a minimal basis set. When combined with an error mitigation scheme,⁴² we obtained results within an accuracy of 10 mhartree.

With the methods presented in this section, the electronic properties (e.g., energies, forces, and non-adiabatic couplings) can be efficiently computed with a quantum processor for a given molecular geometry, that is, for given positions of the nuclei. These can be used to drive classical or quantum trajectories within the so-called trajectory-based quantum dynamics approaches. On the other hand, the PESs required to propagate the nuclear wavepackets (using the Born–Huang expansion) can be obtained by repeating these calculations along the relevant nuclear coordinates. In this case, the quantum advantage will reside in the favorable scaling of encoding the nuclear degrees of freedom (see ref 3). The next section will introduce quantum algorithmic approaches to address this task.

3. QUANTUM ALGORITHMS FOR QUANTUM DYNAMICS SIMULATIONS

Although classical methods such as multiconfigurational time-dependent Hartree (MCTDH) have become incredibly efficient in simulating non-adiabatic dynamics,^{4,43–45} their scaling in the number of nuclear degrees of freedom (DOFs)

remains exponential. On the contrary, simulating quantum dynamics is one of the most promising applications of quantum computing and a vast number of quantum algorithms addressing this problem have been proposed. The choice of algorithm, however, is a delicate question, and in this section, we will give an overview over near- and long-term methods.

3.1. Hamiltonian Simulation with Product Formulas

Let us assume a Hamiltonian of the form $\mathcal{H} = \sum_{j=1}^{N_h} h_j$. The corresponding time propagator, $e^{-i\mathcal{H}t}$, can be approximated with a Lie–Trotter–Suzuki formula.^{20,21,46,47} When t is small and to first order, these product formulas give

$$\exp(-i\mathcal{H}t) = \left(\prod_{j=1}^{N_h} e^{-ih_j(t/d)} \right)^d + O(N_h^2 t^2/d) \quad (4)$$

For Hamiltonians that can be mapped to a qubit lattice with a splitting into even and odd summands, like for the spin-boson Hamiltonian of section 5, the scaling of the error reduces to linear in N_h , $O(N_h t^2/d)$.^{48,49}

The error can also be reduced by increasing the order of the product formula. From a quantum computing perspective, the Trotter approach is employed when $e^{-i\mathcal{H}t}$ cannot exactly be translated into a quantum circuit, but each individual $e^{-ih_j t}$ can. This implies that a decomposition of the Hamiltonian into easily implementable terms is known.

3.2. Hamiltonian Simulation with Variational Quantum Algorithms

The quest for noise resilient quantum dynamics algorithms that can be implemented in near-term (i.e., not error corrected) quantum computers has sparked the development of time-dependent VQAs. These were first proposed by Li et al. in 2017.^{50,51} Generally, a time-dependent variational state $|\Phi(\theta)\rangle$, with $\theta = \theta(t)$, aims to approximate the solution of the TDSE, $|\Psi(t)\rangle$. Preparing such a state on a quantum computer amounts to the action of a parametrized unitary (the quantum circuit) onto a reference qubit-state, $|\Phi(\theta)\rangle = U(\theta)|\phi\rangle$. Since the parameters enter as qubit-gate angles, all parameters must be real.

Our implementation is based on the MVP,¹⁹ which reads

$$\delta \|\langle i | \Theta \rangle - \mathcal{H} |\Phi\rangle\| = 0 \quad (5)$$

where variation is with respect to $|\Theta\rangle = |\dot{\Phi}\rangle$. Equation 5 yields the condition $\mathcal{J}(\delta \Phi | \dot{\Theta} - \mathcal{H} |\Phi\rangle) = 0$. With all time-dependence in θ and including a potential global phase mismatch,⁵¹ $|\Phi\rangle \rightarrow e^{i\alpha(t)}|\Phi\rangle$, we obtain as EOMs

$$\mathcal{M}\dot{\theta} = \mathcal{V} \quad (6)$$

with the matrix elements

$$\mathcal{M}_{ij} = \mathcal{R} \left(\frac{\partial \langle \Phi |}{\partial \theta_i} \frac{\partial | \Phi \rangle}{\partial \theta_j} + \frac{\partial \langle \Phi |}{\partial \theta_i} | \Phi \rangle \frac{\partial \langle \Phi |}{\partial \theta_j} | \Phi \rangle \right) \quad (7)$$

and the vector elements

$$\mathcal{V}_i = \mathcal{J} \left(\frac{\partial \langle \Phi |}{\partial \theta_i} \mathcal{H} | \Phi \rangle - \frac{\partial \langle \Phi |}{\partial \theta_i} | \Phi \rangle \langle \Phi | \mathcal{H} | \Phi \rangle \right) \quad (8)$$

In principle, eq 6 can then be integrated with any numerical ODE-solver. In practice, however, the stability of the dynamics depends on the system investigated and a number of numerical aspects, such as singular value cutoffs and errors associated with numerical integration. In ref 3, we report a detailed study on the influence of quantum hardware noise on the integration of eq 6.

We emphasize that the MVP and the previous derivation are valid for any variational classical or quantum ansatz. What is distinct in the quantum setting is the preparation of the ansatz and the evaluation of individual matrix elements using quantum circuits.^{50,52,53}

For completeness, we also mention (without discussion) other near-term approaches for quantum dynamics, namely, the adaptive variational quantum dynamics simulation,⁵⁴ the subspace variational quantum simulation,⁵⁵ and the variational fast forwarding.⁵⁶

4. GRID-BASED NON-ADIABATIC QUANTUM DYNAMICS

In the previous sections, we presented different approaches for encoding a problem in quantum computers as well as to perform quantum dynamics. In the following, we give a concrete example of the more “long-term” vision. Particularly, in ref 2, we showed how to employ the grid-based quantum encoding discussed in section 2.1 to study the dynamics of a wavepacket on several coupled diabatic surfaces, targeting an exponential advantage compared to the corresponding classical simulation. To be specific, we present our method employing two one-dimensional diabatic curves and the generalization to multiple dimensions is straightforward.

The Hamiltonian of the system is given by

$$\mathcal{H} = K \otimes \mathbf{1} + V_0 \otimes |0\rangle\langle 0| + V_1 \otimes |1\rangle\langle 1| + C \otimes \sigma^x \quad (9)$$

where K is the kinetic energy operator, V_0 and V_1 are the potentials of the first and second diabatic curves, respectively, and C is the coupling operator. The corresponding time propagators act on a $\log_2(N)$ -qubit register, representing N spatial grid points, entangled with an ancilla qubit q_N , which controls the non-adiabatic dynamics across the diabatic curves. q_N is initialized in the state $|0\rangle$ ($|1\rangle$) depending on whether the wavepacket is placed on the first or the second diabatic potential at time $t = 0$. Additionally, an extra qubit register is required to implement C (see below). For concreteness, we specialize to the Marcus model,^{57,58} which provides a simplified description of the electron-transfer reaction rate driven by collective outer and inner sphere coordinates.⁵⁹ In this model the potentials are harmonic and shifted in energy by a given offset as shown in Figure 2a.

Before the dynamics can be simulated, the wavepacket must be initialized in the quantum register. We work with nuclear wavepackets here, meaning the wave function does not need to be antisymmetrized. For the initialization, we rely on a VQE

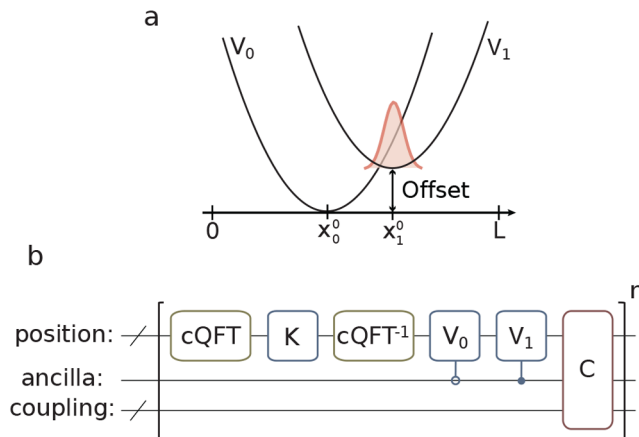


Figure 2. (a) Graphical representation of the Marcus model. (b) Circuit for the time evolution of the wavepacket. The K , V_i , and C blocks represent the time evolution operators for the kinetic, i th potential, and coupling terms, respectively. Reproduced with permission from ref 2. Copyright 2020 American Physical Society.

calculation^{23,24} to prepare the ground state of a harmonic Hamiltonian, $\mathcal{H} = 1/2(p - p_0)^2 + 1/2(x - x_0)^2$, where p and x are the momentum and position operators, respectively, and p_0 and x_0 the initial position and momentum. At each iteration of the VQE, the total energy of the trial wave function, $E = E_{\text{potential}} + E_{\text{kinetic}}$ can be calculated by sampling both in the position and in the momentum basis. For the latter, a centered quantum Fourier transform (cQFT)^{2,60} must be applied before the measurement.

Once initialized, the wavepacket is propagated by applying the Trotterized time evolution operator (cf. section 3.1). A quantum circuit for implementing the time evolution with the kinetic operator and harmonic potentials was presented in refs 61 and 62, and is obtained by discretizing the coordinate x as $x = \sum_{j=0}^{N-1} 2^j k_j$ into the states k_j of N qubits. This formula can be translated to a quantum circuit via the single-qubit rotations

$$U_1(\lambda) = e^{i\lambda/2} R_z(\lambda) = \begin{pmatrix} 1 & 0 \\ 0 & e^{i\lambda} \end{pmatrix} \quad (10)$$

Indeed, the propagator $e^{-i\lambda t}$ can be decomposed into a product of operators $e^{-i\lambda/k_j t}$ equivalent to the above U_1 gate applied to qubit j . The same idea can be employed for executing polynomial functions of x as the single-qubit gates can be replaced by controlled multiqubit operations. The kinetic part of the operator is applied similarly in the momentum space, after performing a cQFT to transition to the momentum basis. While the quantum circuit for the kinetic part of the evolution can be directly applied to the first N qubits, the potential parts must be controlled by the state of the ancilla qubit, q_N , such that the wavepacket evolves under the action of $e^{-iV_0 t/n}$ or $e^{-iV_1 t/n}$ when q_N is in the state $|0\rangle$ or $|1\rangle$, respectively.

One of the main methodological novelties of our approach resides in the encoding of the coupling operator, which corresponds to a rotation of the ancilla qubit around the x -axis by an angle proportional to the coupling function, $f(x)$. To avoid an exponential scaling in the quantum resources,⁶³ $f(x)$ is approximated as a piece-wise linear function.⁶⁴ Importantly, we observe that only a few pieces suffice to obtain accurate results. The full quantum circuit is summarized in a graphical representation shown in Figure 2b.

We computed the dynamics of a wavepacket initialized on V_1 for various offset values (Figure 2a). The simulations were run with a classical emulation of the quantum circuit (dots) and compared to the exact evolution with both a full Gaussian coupling (full lines) and its piece-wise approximation (dashed lines). The piece-wise approximation of the coupling function together with the use of the truncated Trotter expansion of the time-evolution operator lead to the deviations from the exact curve observed in Figure 2a. Here, the population fraction P_0 in the product well V_0 was computed from the expectation value of the ancilla qubit as $P_0 = (\langle \sigma_{qN}^z \rangle + 1)/2$. The initial rate constants (obtained as the slope of linearly fitting the first ten steps of the dynamics, as shown in Figure 3b) resulting from our simulations recover the expected volcano shape behavior predicted by Marcus theory (Figure 3c).

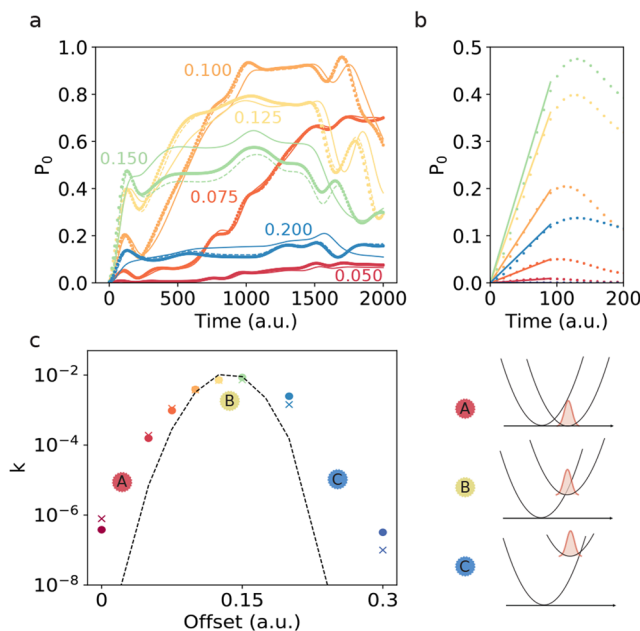


Figure 3. (a) Time evolution of P_0 (see main text) obtained with our algorithm in classical simulations (dots), showing the exact evolution with the reference coupling (full lines), and the exact evolution with the approximate coupling (dashed lines). Colors represent different offset values between V_0 and V_1 . (b) Linear fitting of the ten first steps of the evolution to approximate the rate constants. (c) Approximate rate constants, k , as a function of the offset obtained with our algorithm (dots) and from the exact evolution with the reference coupling (crosses). The Marcus rates are shown as a dashed line for a qualitative comparison. The colored stickers label different charge transfer regions (A, normal regime; B, at reorganization energy; C, inverted region). Reproduced with permission from ref 2. Copyright 2020 American Physical Society.

Although this approach is simple with, in principle, a clear exponential advantage regarding memory, the encodings of arbitrary potentials and couplings remain challenging. Moreover, the large number of queries to one Trotter step leads to very deep quantum circuits, which are far beyond the capacities of current quantum computers. In the following section, we present an opposite vision of quantum algorithms for Hamiltonian simulation, a near-term approach, but with ambiguous quantum advantage.

5. QUANTUM DYNAMICS OF THE SPIN-BOSON MODEL

While the gate-based implementation of the exponential of a Hamiltonian with arbitrary potentials and couplings in first quantization is a nontrivial task, most limitations can be overcome in the second quantization framework by introducing appropriate basis functions.⁶⁵ In fact, alternative to the grid-based approach of section 4, it is straightforward to rewrite the Hamiltonian of eq 9 in second quantization. Furthermore, as eluded to in previous sections, Trotter evolution is typically far too resource-intensive for applications on currently existing, near-term quantum hardware, while time-dependent VQAs appear as resource-efficient alternatives. Hence, complementary to the grid-based approach studied with Trotter evolution, in ref 3, we studied the problem of section 4 in second quantization using a VQA as depicted in Figure 4b.

With harmonic potentials and a coupling $C = f(x) \propto x$, eq 9 can be rewritten as the second-quantized Hamiltonian of a two-level system (the spin) coupled to M bosonic modes (harmonic oscillators),^{66–68}

$$\mathcal{H} = \sum_{k=1}^M \omega_k a_k^\dagger a_k + \frac{\epsilon}{2} \sigma^z + \Delta \sigma^x + \sum_{k=1}^M g_k \sigma^x (a_k^\dagger + a_k) \quad (11)$$

Here, bosonic modes with eigenfrequencies ω_k are created (annihilated) by a_k^\dagger (a_k) and couple to the spin with strength g_k whereas Pauli matrices σ^μ , $\mu \in \{x, y, z\}$, act on the spin-state with eigenfrequency ϵ and tunneling rate Δ .

As outlined in section 2.1, basis states and operators must be mapped to a suitable qubit representation maintaining the correct spin statistics. The state of the spin can be straightforwardly encoded in a single qubit. In the direct mapping,⁶⁹ each bosonic mode's occupation number vector (ONV) is truncated at a maximum excitation n_k^{\max} (cf. Figure 4a) and mapped to an $n_k^{\max} + 1$ qubit register, $|n_k\rangle \rightarrow |\tilde{n}_k\rangle = |0_{n_k^{\max}} \dots 0_{n_{k+1}} 1_{n_k} 0_{n_{k-1}} \dots 0_{n_1}\rangle$. Operators must obey bosonic spin-statistics, leading to $a_k^\dagger \rightarrow \tilde{a}_k^\dagger = \sum_{n_k=0}^{n_k^{\max}-1} \sqrt{n_k + 1} \sigma_{n_k}^+ \sigma_{n_k+1}^-$ and analogously for a_k where $\sigma_{n_k}^\pm = (\sigma_{n_k}^x \pm i\sigma_{n_k}^y)/2$.

Crucially, the choice of variational ansatz heavily impacts resulting performance and accuracy. We use a variational Hamiltonian ansatz (VHA),⁷⁰ closely resembling the unitary time-evolution operator but with the time simply replaced by distinct variational parameters for each term in the Hamiltonian,

$$U_{\mathcal{H}}(\theta) = \exp \left(-i \left[\sum_{k=1}^M \theta_k^{(1)} a_k^\dagger a_k + \theta^{(2)} \sigma^z + \theta^{(3)} \sigma^x + \sigma^x \sum_{k=1}^M \theta_k^{(4)} (a_k + a_k^\dagger) \right] \right) \quad (12)$$

The resulting qubit-mapped exponential is approximately expanded into product form using a Trotter series with d circuit layers, suitable for implementation in terms of one- and two-qubit gates.

In the following, we summarize the findings of ref 3, focusing on the robustness and versatility of algorithm and ansatz as well as its scalability compared to Trotter evolution. We simulated the dynamics of eq 11 in the resonant case, $\omega_k \equiv \omega$

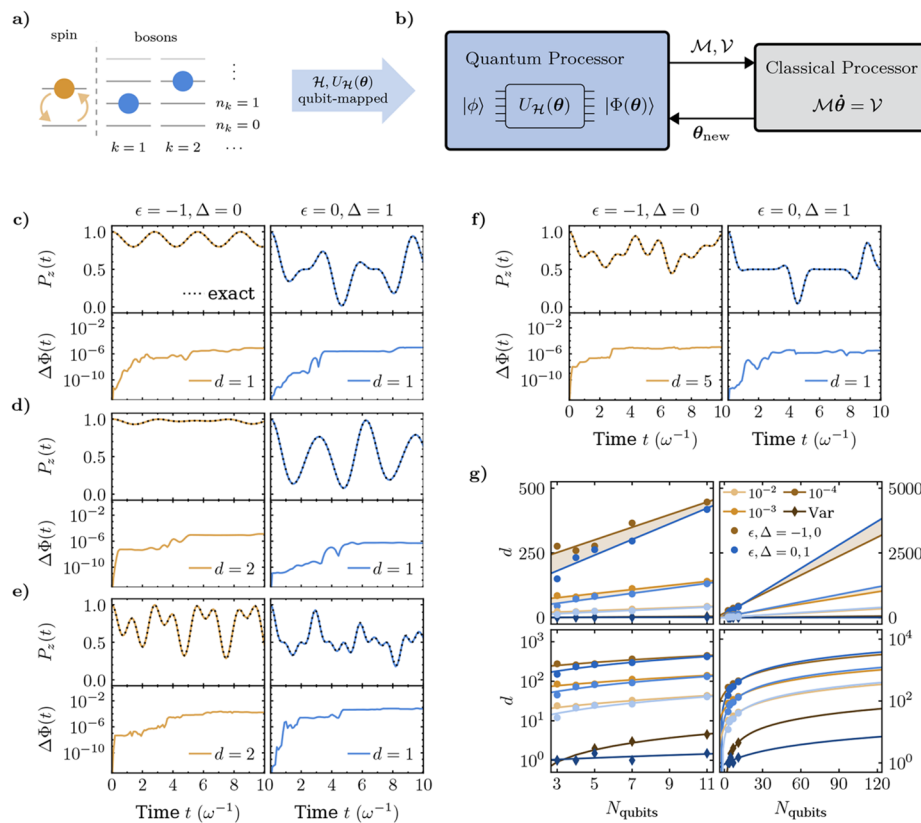


Figure 4. (a) Schematic of the qubit mapping, with a single qubit representing the spin and one qubit for each bosonic n_k . (b) Variational quantum algorithm (VQA) for quantum dynamics. (c–f) Variational simulation results for different system sizes and Hamiltonian parameters, (c) $M = 1$, $n_k^{\max} = 1$, $g/\omega = 0.5$, (d) $M = 2$, $n_k^{\max} = 1$, $g/\omega = 0.2$, (e) $M = 2$, $n_k^{\max} = 1$, $g/\omega = 1.0$, and (f) $M = 5$, $n_k^{\max} = 1$, $g/\omega = 0.5$. The minimum number of circuit layers, d , required to reproduce the correct dynamics is indicated in each subplot. (g) Comparison of the number of circuit layers for the variational algorithm (diamonds) and Trotter evolution (dots) and extrapolation of the scaling to larger qubit numbers (fit lines).

and $g_k \equiv g$, for various Hamiltonian parameter regimes, $(\epsilon, \Delta) \in \{(-1, 0), (0, 1)\}$, and coupling strengths $g/\omega \in [0.1, 1]$ (ultrastrong coupling). The initial qubit state is prepared in the noninteracting ground state of eq 11. We use the infidelity of the approximate state, $\Delta\Phi(t) = 1 - |\langle \Phi | \Psi \rangle|$, as a measure for accuracy and monitor the spin orientation, $P_z = \langle \sigma^z + 1 \rangle / 2$, throughout each simulation.

Figure 4c–f displays simulation outcomes obtained from variational simulation of different system sizes. The respective legends report the minimal numbers of circuit layers in the Trotter expansion of the ansatz, d , necessary to reproduce the correct dynamics. These results emphasize the flexibility of our ansatz to resemble various system setups with far less than exponentially many DOFs, which becomes evident as the number of variational parameters scales linearly with the system size, $N_\theta = 2d(Mn^{\max} + 1)$. For instance, $N_\theta = 6$ ($d = 1$) and $N_\theta = 12$ ($d = 2$) parameters in the 5-qubit case. Note that the results presented here are noise-free. A series of simulations including the realistic hardware noise of IBM's quantum computer *ibmq_santiago*⁴¹ was presented in ref 3.

Furthermore, we performed a comparative study between variational and Trotter simulation. The applicability of Trotter evolution is mainly limited by a rapidly increasing circuit depth, quickly exceeding the capabilities of today's available quantum hardware. Hence, in Figure 4g, we compare the final number of circuit layers required by Trotter simulation to reach a target accuracy $\Delta\Phi < \epsilon \in \{10^{-4}, 10^{-3}, 10^{-2}\}$ (see legend) as a function of system size and compare to that of the

variational approach for $\epsilon = 10^{-4}$. Importantly, the circuit depth is fixed throughout the variational simulation, whereas it increases with simulation time during Trotter evolution. The data obtained with both simulation methods was fitted linearly (cf. lines in Figure 4g). In this way, we could extrapolate the observed scaling to system sizes currently out of reach for both classical and quantum computers. Evidently, the variational approach required far fewer circuit layers than Trotter simulation. This, however, has to be put in relation to the additional cost associated with the circuit evaluations in the variational approach.

Given a storage of 10^{12} bits (as available on a state-of-the-art supercomputer) one could store the wave function of, for example, 12 bosonic modes with 10 DOFs per mode ($M = 12$, $n^{\max} = 9$). With the methods discussed here, this corresponds to 121 qubits. Keeping the simulation error $\epsilon < 10^{-4}$ and extrapolating the above fit results, Trotter evolution necessitates roughly $d = 3400$ circuit layers. Taking into account the time needed to execute each gate in a layer, this amounts to approximately 1 s compute time to reach the final simulation time.

Analyzing the cost of the variational approach, one needs to account for classical contributions given by the number of time steps, and the cost at each time step, determined by the number of parameters, which is linear in system size. Further, quantum contributions to the cost arise from the time taken per circuit execution, which is obtained analogous to the cost for Trotter evolution, as well as the number of circuit

evaluations to populate matrix and vector in the EOM, [eq 6](#), at each time step. All this combined results in a total of $N_{\text{circ}} \approx 10^{18}$ circuit evaluations, amounting to roughly $10^{15} \text{ s} \approx 3 \times 10^7 \text{ yr}$ for a 121-qubit simulation.

6. CONCLUSIONS AND OUTLOOK

In summary, molecular quantum simulations are challenging due to the unfavorable scaling of the classical algorithms with the dimensionality of the problem. In a quest for finding methods to improve the efficiency and quality of large scale computations, quantum algorithms appear as an interesting path to pursue. This rather new area of research has already led to several different approaches to tackle the simulation of molecular quantum dynamics.^{2,3}

In this Account, we gave an overview of various such methods and showed how they apply and compare in concrete physical examples. While the theoretical advantage associated with the polynomial encoding of the molecular DOFs is evident for both electronic and nuclear components, there remain important technical issues that hamper the use of quantum computers for solving time-dependent problems of this complexity. Our results highlight the need for quantum hardware on which long circuits (with a coherence time on the order of seconds) can be executed with high fidelity. Moreover, additional efforts must be made for designing algorithms with the right trade-off between circuit depth and the number of measurements (or parallelizable parts). Since the computational bottleneck does not reside in the memory of quantum computers, we expect that the simultaneous treatment of both electrons and nuclei, in the adiabatic and non-adiabatic regimes, will follow once the necessary technological developments for near-term (i.e., error mitigated) and fault-tolerant (i.e., error corrected) quantum computers will become available.

■ AUTHOR INFORMATION

Corresponding Author

Ivano Tavernelli – IBM Quantum, IBM Research–Zürich, 8803 Rüschlikon, Switzerland;  orcid.org/0000-0001-5690-1981; Email: ita@zurich.ibm.com

Authors

Pauline J. Ollitrault – IBM Quantum, IBM Research–Zürich, 8803 Rüschlikon, Switzerland

Alexander Miessen – IBM Quantum, IBM Research–Zürich, 8803 Rüschlikon, Switzerland

Complete contact information is available at:
<https://pubs.acs.org/10.1021/acs.accounts.1c00514>

Author Contributions

[†]P.J.O. and A.M. contributed equally to this work.

Notes

The authors declare no competing financial interest.

Biographies

Pauline Ollitrault became a research staff member at IBM Quantum, IBM Research–Zürich, after completing her Ph.D. in Chemistry jointly between IBM Research and ETH Zürich (ETHZ). She is interested in applications of quantum computers to chemistry problems such as electronic and vibrational structure calculations, as well as quantum dynamics.

Alexander Miessen is a research intern at IBM Quantum, IBM Research–Zürich. He holds a Master in physics from ETHZ and is interested in near-term applications of quantum computers to the simulation of quantum many-body dynamics.

Ivano Tavernelli is a Research Staff Member in Quantum Technology at IBM Research–Zurich. Since 2018, he is responsible for the development of quantum algorithms and applications in chemistry, physics, and material science at IBM. His focus is the design of efficient and scalable quantum algorithms for near-term and fault-tolerant quantum computers. He holds two masters (Biochemistry and Theoretical Physics) and a doctorate in theoretical biophysics from ETHZ.

■ ACKNOWLEDGMENTS

The authors acknowledge financial support from the Swiss National Science Foundation (SNF) through Grant No. 200021-179312. IBM, the IBM logo, and [ibm.com](https://www.ibm.com) are trademarks of International Business Machines Corp., registered in many jurisdictions worldwide. Other product and service names might be trademarks of IBM or other companies. The current list of IBM trademarks is available at <https://www.ibm.com/legal/copytrade>.

■ REFERENCES

- (1) Ollitrault, P. J.; Kandala, A.; Chen, C.-F.; Barkoutsos, P. K.; Mezzacapo, A.; Pistoia, M.; Sheldon, S.; Woerner, S.; Gambetta, J. M.; Tavernelli, I. Quantum equation of motion for computing molecular excitation energies on a noisy quantum processor. *Phys. Rev. Res.* **2020**, *2*, 043140.
- (2) Ollitrault, P. J.; Mazzola, G.; Tavernelli, I. Nonadiabatic Molecular Quantum Dynamics with Quantum Computers. *Phys. Rev. Lett.* **2020**, *125*, 260511.
- (3) Miessen, A.; Ollitrault, P. J.; Tavernelli, I. Quantum algorithms for quantum dynamics: a performance study on the spin-boson model, *arXiv preprint*, 2021, arXiv:2108.04258, <https://arxiv.org/abs/2108.04258>.
- (4) Meyer, H. D.; Gatti, F.; Worth, G. A. *Multidimensional Quantum Dynamics: MCTDH Theory and Applications*; John Wiley & Sons, Ltd, 2009; pp 1–419.
- (5) Tully, J. C.; Preston, R. K. Trajectory Surface Hopping Approach to Nonadiabatic Molecular Collisions: The Reaction of H⁺ with D₂. *J. Chem. Phys.* **1971**, *55*, 562.
- (6) Curchod, B. F. E.; Rothlisberger, U.; Tavernelli, I. Trajectory-based nonadiabatic dynamics with time-dependent density functional theory. *ChemPhysChem* **2013**, *14*, 1314.
- (7) Curchod, B. F.; Martínez, T. J. Ab initio nonadiabatic quantum molecular dynamics. *Chem. Rev.* **2018**, *118*, 3305.
- (8) Gatti, F. *Molecular quantum dynamics: from theory to applications*; Springer, 2014.
- (9) Abedi, A.; Maitra, N. T.; Gross, E. K. U. Exact factorization of the time-dependent electron-nuclear wave function. *Phys. Rev. Lett.* **2010**, *105*, 123002.
- (10) Min, S. K.; Agostini, F.; Tavernelli, I.; Gross, E. K. U. Ab initio nonadiabatic dynamics with coupled trajectories: A rigorous approach to quantum (de)coherence. *J. Phys. Chem. Lett.* **2017**, *8*, 3048.
- (11) Nielsen, M. A.; Chuang, I. L. *Quantum Computation and Quantum Information*, 10th ed.; Cambridge University Press: Cambridge, MA, USA, 2011.
- (12) Cao, Y.; Romero, J.; Olson, J. P.; Degroote, M.; Johnson, P. D.; Kieferová, M.; Kivlichan, I. D.; Menke, T.; Peropadre, B.; Sawaya, N. P.; Sim, S.; Veis, L.; Aspuru-Guzik, A. Quantum Chemistry in the Age of Quantum Computing. *Chem. Rev.* **2019**, *119*, 10856.
- (13) Barkoutsos, P. K.; Gonthier, J. F.; Sokolov, I.; Moll, N.; Salis, G.; Fuhrer, A.; Ganzhorn, M.; Egger, D. J.; Troyer, M.; Mezzacapo, A.; Filipp, S.; Tavernelli, I. Quantum algorithms for electronic

structure calculations: Particlehole Hamiltonian and optimized wavefunction expansions. *Phys. Rev.* **2018**, *98*, 022322.

(14) O’Malley, P. J. J.; Babbush, R.; Kivlichan, I. D.; Romero, J.; McClean, J. R.; Barends, R.; Kelly, J.; Roushan, P.; Tranter, A.; Ding, N.; Campbell, B.; Chen, Y.; Chen, Z.; Chiaro, B.; Dunsworth, A.; Fowler, A. G.; Jeffrey, E.; Lucero, E.; Megrant, A.; Mutus, J. Y.; Neeley, M.; Neill, C.; Quintana, C.; Sank, D.; Vainsencher, A.; Wenner, J.; White, T. C.; Coveney, P. V.; Love, P. J.; Neven, H.; Aspuru-Guzik, A.; Martinis, J. M. Scalable quantum simulation of molecular energies. *Phys. Rev. X* **2016**, *6*, 031007.

(15) Kandala, A.; Mezzacapo, A.; Temme, K.; Takita, M.; Brink, M.; Chow, J. M.; Gambetta, J. M. Hardware-efficient variational quantum eigensolver for small molecules and quantum magnets. *Nature* **2017**, *549*, 242.

(16) Suchsland, P.; Barkoutsos, P. K.; Tavernelli, I.; Fischer, M. H.; Neupert, T. Simulating a ring-like Hubbard system with a quantum computer, *arXiv preprint*, 2021, arXiv:2104.06428, <https://arxiv.org/abs/2104.06428>.

(17) Babbush, R.; Wiebe, N.; McClean, J.; McClain, J.; Neven, H.; Chan, G. K.-L. Low-depth quantum simulation of materials. *Phys. Rev. X* **2018**, *8*, 011044.

(18) Sokolov, I. O.; Barkoutsos, P. K.; Moeller, L.; Suchsland, P.; Mazzola, G.; Tavernelli, I. Microcanonical and finite-temperature ab initio molecular dynamics simulations on quantum computers. *Phys. Rev. Res.* **2021**, *3*, 013125.

(19) McLachlan, A. D. A variational solution of the time-dependent Schrödinger equation. *Mol. Phys.* **1964**, *8*, 39.

(20) Trotter, H. F. On the product of semi-groups of operators. *Proc. Am. Math. Soc.* **1959**, *10*, 545.

(21) Suzuki, M. Generalized trotter’s formula and systematic approximants of exponential operators and inner derivations with applications to many-body problems. *Commun. Math. Phys.* **1976**, *51*, 183.

(22) Kassal, I.; Whitfield, J. D.; Perdomo-Ortiz, A.; Yung, M.-H.; Aspuru-Guzik, A. Simulating chemistry using quantum computers. *Annu. Rev. Phys. Chem.* **2011**, *62*, 185.

(23) Peruzzo, A.; McClean, J.; Shadbolt, P.; Yung, M. H.; Zhou, X. Q.; Love, P. J.; Aspuru-Guzik, A.; O’Brien, J. L. A variational eigenvalue solver on a photonic quantum processor. *Nat. Commun.* **2014**, *5*, 4213.

(24) McClean, J. R.; Romero, J.; Babbush, R.; Aspuru-Guzik, A. The theory of variational hybrid quantumclassical algorithms. *New J. Phys.* **2016**, *18*, 023023.

(25) Mitarai, K.; Nakagawa, Y. O.; Mizukami, W. Theory of analytical energy derivatives for the variational quantum eigensolver. *Phys. Rev. Res.* **2020**, *2*, 013129.

(26) O’Brien, T. E.; Senjean, B.; Sagastizabal, R.; Bonet- Monroig, X.; Dutkiewicz, A.; Buda, F.; DiCarlo, L.; Visscher, L. Calculating energy derivatives for quantum chemistry on a quantum computer. *npj Quantum Inf.* **2019**, *5*, 113.

(27) Romero, J.; Babbush, R.; McClean, J. R.; Hempel, C.; Love, P. J.; Aspuru-Guzik, A. Strategies for quantum computing molecular energies using the unitary coupled cluster ansatz. *Quantum Sci. Technol.* **2019**, *4*, 014008.

(28) Grimsley, H. R.; Claudino, D.; Economou, S. E.; Barnes, E.; Mayhall, N. J. Is the trotterized uccsd ansatz chemically well-defined? *J. Chem. Theory Comput.* **2020**, *16*, 1.

(29) Evangelista, F. A.; Chan, G. K.-L.; Scuseria, G. E. Exact parameterization of fermionic wave functions via unitary coupled cluster theory. *J. Chem. Phys.* **2019**, *151*, 244112.

(30) Bartlett, R. J.; Musiał, M. Coupled-cluster theory in quantum chemistry. *Rev. Mod. Phys.* **2007**, *79*, 291.

(31) Sokolov, I. O.; Barkoutsos, P. K.; Ollitrault, P. J.; Greenberg, D.; Rice, J.; Pistoia, M.; Tavernelli, I. Quantum orbital-optimized unitary coupled cluster methods in the strongly correlated regime: Can quantum algorithms outperform their classical equivalents? *J. Chem. Phys.* **2020**, *152*, 124107.

(32) Lee, J.; Huggins, W. J.; Head-Gordon, M.; Whaley, B. K. Generalized unitary coupled cluster wave functions for quantum computation. *J. Chem. Theory Comput.* **2019**, *15*, 311.

(33) Mizukami, W.; Mitarai, K.; Nakagawa, Y. O.; Yamamoto, T.; Yan, T.; Ohnishi, Y.-y. Orbital optimized unitary coupled cluster theory for quantum computer. *Phys. Rev. Res.* **2020**, *2*, 033421.

(34) Grimsley, H. R.; Economou, S. E.; Barnes, E.; Mayhall, N. J. An adaptive variational algorithm for exact molecular simulations on a quantum computer. *Nat. Commun.* **2019**, *10*, 3007.

(35) Mazzola, G.; Ollitrault, P. J.; Barkoutsos, P. K.; Tavernelli, I. Nonunitary operations for ground-state calculations in near-term quantum computers. *Phys. Rev. Lett.* **2019**, *123*, 130501.

(36) Santagati, R.; Wang, J.; Gentile, A. A.; Paesani, S.; Wiebe, N.; McClean, J. R.; Morley-Short, S.; Shadbolt, P. J.; Bonneau, D.; Silverstone, J. W.; Tew, D. P.; Zhou, X.; O’Brien, J. L.; Thompson, M. G. Witnessing eigenstates for quantum simulation of hamiltonian spectra. *Sci. Adv.* **2018**, *4*, eaap9646.

(37) Higgott, O.; Wang, D.; Brierley, S. Variational Quantum Computation of Excited States. *Quantum* **2019**, *3*, 156.

(38) Chan, H. H. S.; Fitzpatrick, N.; Segarra-Martí, J.; Bearpark, M. J.; Tew, D. P. Molecular excited state calculations with adaptive wavefunctions on a quantum eigensolver emulation: Reducing circuit depth and separating spin states, *arXiv preprint*. 2021, arXiv:2105.10275, <https://arxiv.org/abs/2105.10275>.

(39) McClean, J. R.; Kimchi-Schwartz, M. E.; Carter, J.; de Jong, W. A. Hybrid quantum-classical hierarchy for mitigation of decoherence and determination of excited states. *Phys. Rev. A* **2017**, *95*, 042308.

(40) Colless, J. I.; Ramasesh, V. V.; Dahlen, D.; Blok, M. S.; Kimchi-Schwartz, M. E.; McClean, J. R.; Carter, J.; de Jong, W. A.; Siddiqi, I. Computation of molecular spectra on a quantum processor with an error-resilient algorithm. *Phys. Rev. X* **2018**, *8*, 011021.

(41) IBM Quantum, <https://quantum-computing.ibm.com/>, 2021 (accessed 16.06.2021).

(42) Kandala, A.; Temme, K.; Córcoles, A. D.; Mezzacapo, A.; Chow, J. M.; Gambetta, J. M. Error mitigation extends the computational reach of a noisy quantum processor. *Nature* **2019**, *567*, 491.

(43) Burghardt, I.; Giri, K.; Worth, G. A. Multimode quantum dynamics using Gaussian wavepackets: The Gaussian-based multi-configuration time-dependent Hartree (G-MCTDH) method applied to the absorption spectrum of pyrazine. *J. Chem. Phys.* **2008**, *129*, 174104.

(44) Meng, Q.; Meyer, H.-D. A multilayer mctdh study on the full dimensional vibronic dynamics of naphthalene and anthracene cations. *J. Chem. Phys.* **2013**, *138*, 014313.

(45) Picconi, D.; Burghardt, I. Time-resolved spectra of I2 in a krypton crystal by G-MCTDH simulations: Nonadiabatic dynamics, dissipation and environment driven decoherence. *Faraday Discuss.* **2020**, *221*, 30.

(46) Berry, D. W.; Ahokas, G.; Cleve, R.; Sanders, B. C. Efficient quantum algorithms for simulating sparse hamiltonians. *Commun. Math. Phys.* **2007**, *270*, 359.

(47) Dür, W.; Bremner, M. J.; Briegel, H. J. Quantum simulation of interacting high-dimensional systems: The influence of noise. *Phys. Rev. A* **2008**, *78*, 052325.

(48) Chiesa, A.; Tacchino, F.; Grossi, M.; Santini, P.; Tavernelli, I.; Gerace, D.; Carretta, S. Quantum hardware simulating four-dimensional inelastic neutron scattering. *Nat. Phys.* **2019**, *15*, 455.

(49) Childs, A. M.; Su, Y. Nearly Optimal Lattice Simulation by Product Formulas. *Phys. Rev. Lett.* **2019**, *123*, 050503.

(50) Li, Y.; Benjamin, S. C. Efficient Variational Quantum Simulator Incorporating Active Error Minimization. *Phys. Rev. X* **2017**, *7*, 021050.

(51) Yuan, X.; Endo, S.; Zhao, Q.; Li, Y.; Benjamin, S. C. Theory of variational quantum simulation. *Quantum* **2019**, *3*, 191.

(52) Somma, R.; Ortiz, G.; Gubernatis, J. E.; Knill, E.; Laflamme, R. Simulating physical phenomena by quantum networks. *Phys. Rev. A* **2002**, *65*, 042323.

(53) Schuld, M.; Bergholm, V.; Gogolin, C.; Izaac, J.; Killoran, N. Evaluating analytic gradients on quantum hardware. *Phys. Rev. A* **2019**, *99*, 032331.

(54) Bharti, K.; Haug, T. Quantum Assisted Simulator. *Phys. Rev. A* **2021**, *104* (4), 042418.

(55) Heya, K.; Nakanishi, K. M.; Mitarai, K.; Fujii, K. Subspace Variational Quantum Simulator, *arXiv preprint*, 2019, arXiv:1904.08566, <https://arxiv.org/abs/1904.08566>.

(56) Cirstoiu, C.; Holmes, Z.; Iosue, J.; Cincio, L.; Coles, P. J.; Sornborger, A. Variational fast forwarding for quantum simulation beyond the coherence time. *npj Quantum Inf.* **2020**, *6*, 82.

(57) Marcus, R. A. Chemical and electrochemical electrontransfer theory. *Annu. Rev. Phys. Chem.* **1964**, *15*, 155.

(58) Marcus, R. A. Electron transfer reactions in chemistry. theory and experiment. *Rev. Mod. Phys.* **1993**, *65*, 599.

(59) Siders, P.; Marcus, R. A. Quantum effects for electrontransfer reactions in the “inverted region”. *J. Am. Chem. Soc.* **1981**, *103*, 748.

(60) Nielsen, M. A.; Chuang, I. *Quantum computation and quantum information* Cambridge University Press, 2002.

(61) Benenti, G.; Strini, G. Quantum simulation of the single-particle schrödinger equation. *Am. J. Phys.* **2008**, *76*, 657.

(62) Somma, R. D. Quantum simulations of one dimensional quantum systems, *arXiv preprint*, 2015, arXiv:1503.06319v2, <https://arxiv.org/abs/1503.06319>.

(63) Mitarai, K.; Kitagawa, M.; Fujii, K. Quantum analogdigital conversion. *Phys. Rev. A* **2019**, *99*, 012301.

(64) Häner, T.; Roetteler, M.; Svore, K. M. Optimizing quantum circuits for arithmetic, *arXiv preprint*, 2018, arXiv:1805.12445, <https://arxiv.org/abs/1805.12445>.

(65) Ollitrault, P. J.; Baiardi, A.; Reiher, M.; Tavernelli, I. Hardware efficient quantum algorithms for vibrational structure calculations. *Chem. Sci.* **2020**, *11*, 6842.

(66) Frisk Kockum, A.; Miranowicz, A.; De Liberato, S.; Savasta, S.; Nori, F. Ultrastrong coupling between light and matter. *Nat. Rev. Phys.* **2019**, *1*, 19.

(67) Di Paolo, A.; Barkoutsos, P. K.; Tavernelli, I.; Blais, A. Variational Quantum Simulation of Ultrastrong Light- Matter Coupling. *Phys. Rev. Res.* **2020**, *2*, 033364.

(68) Tong, Z.; Gao, X.; Cheung, M. S.; Dunietz, B. D.; Geva, E.; Sun, X. Charge transfer rate constants for the carotenoid-porphyrin-C₆₀molecular triad dissolved in tetrahydrofuran: The spin-boson model vs the linearized semiclassical approximation. *J. Chem. Phys.* **2020**, *153*, 044105.

(69) Somma, R.; Ortiz, G.; Knill, E.; Gubernatis, J. Errata: Quantum Simulations of Physics Problems. *Int. J. Quantum Inf.* **2003**, *01*, 417.

(70) Wecker, D.; Hastings, M. B.; Troyer, M. Progress towards practical quantum variational algorithms. *Phys. Rev. A* **2015**, *92*, 042303.